Here, there and everywhere. A multi organ approach to acylcarnitine metabolism

Schooneman, M.G.

Publication date
2015

Document Version
Final published version

C5

Acylcarnitine kinetics in a fasting- and obesity-induced insulin resistant mouse model

Marieke G. Schooneman, Sander M. Houten, Nicolaas E.P. Deutz, Maarten R. Soeters

Submitted

Abstract

Acylcarnitines are derived from mitochondrial acyl-CoA metabolism, and have been studied in relation to diet-induced insulin resistance. Acylcarnitine kinetics, such as production rates and pool sizes, may aid in the understanding of the role of acylcarnitines under different metabolic circumstances. We aimed to determine acylcarnitine kinetics in various mouse models of insulin resistance.

We studied 12 lean BALB/cJ mice and 10 lean versus 10 obese C57BL/6N mice. We infused a bolus of U-13C-C16-carnitine, and one week later D3-C2-carnitine in fasted and fed mice, either fed chow or high fat diet (HFD). Blood was sampled for up to 180 minutes, and after calculation of isotope enrichment, non-compartmental analysis was done.

Both C2- and C16-carnitine kinetics allow single pool model analysis. A larger C16-carnitine pool size was found in BALB/cJ mice ($p=0.017$), but other kinetics were comparable. In C57BL/6N mice, both fasting and HFD did not affect C16-carnitine kinetics. In contrast, C2-carnitine pool size and rate of appearance (Ra) were greater in fasted chow mice ($p=0.007$), along with a lower elimination constant k ($p=0.016$). A lower C2-carnitine Ra was found during HFD ($p=0.02$).

C2 and C16-carnitine kinetics can be analysed with a single pool model. Our results suggest that HFD alters mainly C2-carnitine metabolism. We speculate that these findings reflect impaired substrate switching in HFD-induced insulin resistance.

Introduction

Acylcarnitines are fatty acid oxidation (FAO) intermediates that are studied extensively in relation to fatty acid oxidation disorders (1-4), and more recently in relation to diet-induced metabolic derangements (5-10). For these purposes, acylcarnitines are studied in tissues like heart, liver and skeletal muscle, but many studies mainly focus on plasma acylcarnitine profiles (9, 11). However, we have shown recently that plasma profiles do not reflect tissue acylcarnitine metabolism (12). Only a small fraction of the total acylcarnitine pool is present in plasma, whereas the rest resides in tissues (12, 13). It is unknown how plasma concentrations relate to acylcarnitine transport between plasma and tissues. As only a few organs are capable of carnitine synthesis, and carnitine mainly is absorbed from the diet, an efficient system for transportation and distribution of carnitine and acylcarnitines between tissues and plasma is required.

Liver, kidney and brain are capable of de novo carnitine synthesis, as these organs contain the gamma-butyrobetaine dioxygenase (BBD) enzyme which catalyses the last step of carnitine synthesis from its precursor gamma-butyrobetaine (13). Carnitine is transported into cells via the sodium dependent transporter OCTN2, found in fat oxidizing tissues (14, 15). OCTN2 also transports C2-carnitine and gamma-butyrobetaine with a higher affinity compared to carnitine, and their transport is competitively inhibited by carnitine (15). Once inside the cell, carnitine binds to an activated fatty acid in exchange for CoA by carnitine-palmitoyltransferase 1 (CPT-1) on the outer mitochondrial membrane, and the

resulting acylcarnitine subsequently crosses the mitochondrial inner membrane via the carnitine-acylcarnitine-transporter (CACT). Here, carnitine-palmitoyltransferase 2 (CPT-2) exchanges the FFA again for a CoA, forming acyl-CoA which enters the beta-oxidation for energy production (3, 13).
In the last decade there have been several studies proposing a theory of lipotoxicity, where intracellular lipids cause stress within the cytosol with impairment of the insulin signalling cascade and the induction of insulin resistance (5, 16-18). Within this concept, acylcarnitines were also proposed to interfere with insulin signalling (5, 6, 9). The high lipid flux in obesity could increase rates of incomplete FAO, causing an accumulation of acylcarnitines, which could distort insulin signalling in the cytosol and flow back into the plasma, as reflected by increased plasma acylcarnitine levels in obese, insulin resistant subjects (6, 9). To improve the interpretation of plasma acylcarnitines and how their appearance and concentration relates to the total acylcarnitine pool in tissues, we used stable acylcarnitine isotopes to study these metabolites in vivo as has been done from other metabolic processes in both human and animal studies (19-23). Here C16-carnitine has been related to obesity-induced insulin resistance, whereas C2-carnitine is proposed to play a crucial role in switching between lipid and glucose metabolism (24, 25). We studied acylcarnitine metabolism with the stable isotopes U-13C-C16-carnitine and D3-C2-carnitine in fed and fasted, lean and obese mice. We infused these tracers in both BALB/cJ and C57BL/6N mice that differ in insulin sensitivity (26) to gain more insight in FAO in both insulin sensitivity and insulin resistance.

Methods

Tracer studies in lean mice

Tracer experiments were first performed in 12 lean and insulin sensitive BALB/cJ mice (26), half of which were fasted overnight whereas the other half were fed at libitum. At 8am after the overnight fast, conscious mice were weighed and one baseline blood sample of 10µL was drawn via tail bleeding. After blood sampling, mice were placed in a mouse restrainer and a bolus infusion of 125 µL of U-13C-C16-carnitine solution (1µg/mL in 0.9% NaCl) was injected via the tail vein. Blood was sampled via tail bleeding after 5, 10, 15, 20 and 30 minutes upon infusion. Blood samples of 10 µL were diluted in 90 µL of NaCl with EDTA (5.5 mmol/L in NaCl 0.9%) and directly placed on ice.

Tracer studies in lean versus obese mice

We repeated the experiment in 20 C57BL/6N mice that are more prone to develop insulin resistance (27). Mice were fed either chow or HFD for 8 weeks prior to the isotope infusions. After the diet we first performed an intra-peritoneal glucose tolerance test (IPGTT) to assess the insulin sensitivity upon the high fat diet in comparison with the control group. After an overnight fast (~17 hours), mice were weighed and blood was taken via tail bleeding for a baseline (t=0) blood glucose level measurement (Bayer Contour). Subsequently 2g/kg bodyweight D-glucose (20% D-glucose in 0.9% NaCl) was injected

intraperitoneally. Blood glucose levels were determined after 15, 30, 45, 60, 90 and 120 minutes. Subsequently, one week after the glucose tolerance test, they were infused with U-13C-C16-carnitine and additionally one week later D3-C2-carnitine in fasted versus fed mice. Upon these infusions we prolonged the period of blood sampling which was performed after 15, 30, 45, 60, 90, 120 and 180 minutes, to secure the detection of possible delayed effects after infusion.

Laboratory analyses

For measurement of the tracer/tracee ratio (TTR), we centrifuged the diluted blood samples and transferred 50 µL of diluted plasma into clean tubes. The plasma samples were deproteinized by addition of 500 µl acetonitrile (ACN) and subsequent vortex mixing. Next, samples were centrifuged for 10 minutes at 4°C at a speed of 20,000 g. The supernatant was transferred into 4 ml glass vials and evaporated under a stream of nitrogen at 40°C. After evaporation, the residue was dissolved in 100 µl ACN, vortex mixed and transferred to Gilson vials for HPLC mass spectrometric analysis (Waters/Micromass Quattro Premier XE). TTRs were further calculated by dividing the peak area of the tracer (U-13C-C16- or D3-C2-carnitine) by the peak area of the endogenous tracee (C16- or C2-carnitine).

Calculations and Statistical Analysis

Additional analyses and statistics were performed using Microsoft Excel 2011 version 14.4.4 and Graphpad Prism software version 6.0c. First, Excel was used for the inventory of mouse data, including body weight, bolus infusion volume (absolute and corrected for lean body mass) and the calculation of TTRs. Graphpad was used to generate and fit non-linear regression curves of the individual TTRs.

We determined the proposed model for decay of the curve in Graphpad Prism. From the fitted curves we were able to determine the initial enrichment (Y0) and calculate the estimated pool size (Q), the elimination constant from the pool (k) and the rate of appearance (Ra). We observed that the data were best fitted in a single pool model. Ra was calculated as $Ra = k \cdot Q$ (28).

Q is expressed as µmol/mouse, and the dose was the absolute amount of tracer in µmol, which was infused at time point 0. Additionally we calculated the anticipated Y0 as Tracer dose/Total absolute [C16-carnitine](µmol/mouse). Total absolute [C16-carnitine] was calculated using the anticipated blood volume and lean body mass. Both blood volume and lean body mass are estimates based on the total body mass measured prior to isotope infusion. Mann-Whitney tests were performed to detect effects in the different mouse groups from the fasting or diet intervention. All data are expressed as means ± SEM. P-values < 0.05 are considered as statistically significant and depicted as *, and p-values < 0.01 are depicted as **.

Results

Prior to the tracer infusion studies, we performed an intraperitoneal glucose tolerance test (IPGTT) in the C57BL/6N mice to monitor whether the HFD induced insulin resistance. Indeed, the mice on HFD showed impaired glucose tolerance when compared to the chow fed controls ($p < 0.05$ on all GTT time points, data not shown).

Y0: estimated ratio of enrichment by the tracer on time point zero

We first determined the Y0, the estimated ratio of enrichment by the tracer on time point 0, from the slope of the TTR curves. Y0 values were high in all experiments. In the BALB/cJ mice, the Y0 was overall greater than 1, meaning that the infused amount of tracer exceeded the endogenous plasma pool (figure 1a). The Y0 for C16-carnitine differed significantly between fed and fasted BALB/cJ mice (fed Y0: 4.13 ± 0.78 and fasted Y0: 1.26 ± 0.38, $p=0.01$). Thus, the plasma pool of endogenous C16-carnitine in the fasted state was ~3.3 times greater compared with the fed state.

In the C57BL/6N mice, the Y0 for C16-carnitine was overall greater than 1 as well, and did not differ between all four groups (fed chow: Y0 5.81 ± 1.56; fasted chow: Y0 3.10 ± 0.92; fed HFD: Y0 5.44 ± 0.20; and fasted HFD: Y0 3.11 ± 0.81). This shows that fasting and HFD do not alter the endogenous C16-carnitine pool size of C57BL/6N mice opposed to BALB/cJ mice (figure 1b).

The C2-carnitine Y0 of the chow fed C57BL/6N mice was much lower and did differ significantly between fed and fasted C57BL/6N mice (fed chow: Y0 1.59 ± 0.27 versus fasted chow: Y0 0.40 ± 0.06, $p=0.008$) but not in the HFD group (fed HFD: Y0 1.28 ± 0.36 versus fasted Y0 mean TTR 1.16 ± 0.74) (figure 1c). Apparently, fasting induces a rise in the C2-carnitine concentration in lean mice as reflected by the lower Y0, which does not occur in HFD-fed obese mice. This corresponds with the results from our earlier study in which fasting induced a rise in the plasma C2-carnitine concentration in lean C57BL/6N mice and BALB/cJ mice (12).

Anticipated and actual pool size (Q)

First we calculated the anticipated pool size for all mice by dividing the tracer dose by the anticipated Y0 value. When the actual pool size is compared with the anticipated pool size, we found that the actual pool is much larger (data not shown). The anticipated pool size is an estimate of the pool present in the plasma compartment. This difference between this estimated plasma pool size and the total pool residing in tissue, is consistent with the difference in measured concentrations of C2-carnitine and C16-carnitine in both plasma and tissues of fasted and fed BALB/cJ and C57BL/6N mice (12). We have calculated the ratios between the actual pool size and the anticipated pool size of C16-carnitine and C2-carnitine (Supplemental figure S1a and S1b). For C16-carnitine we found ratios ranging from 5 in fed BALB/cJ mice to 48 in fasted BALB/cJ mice. In agreement with the pool sizes, ratios were overall much greater in fasted mice (Supplemental figure S1a), indicating that a greater pool size in plasma is accompanied by a greater fast-exchanging pool outside of the plasma as well. The ratio differed significantly

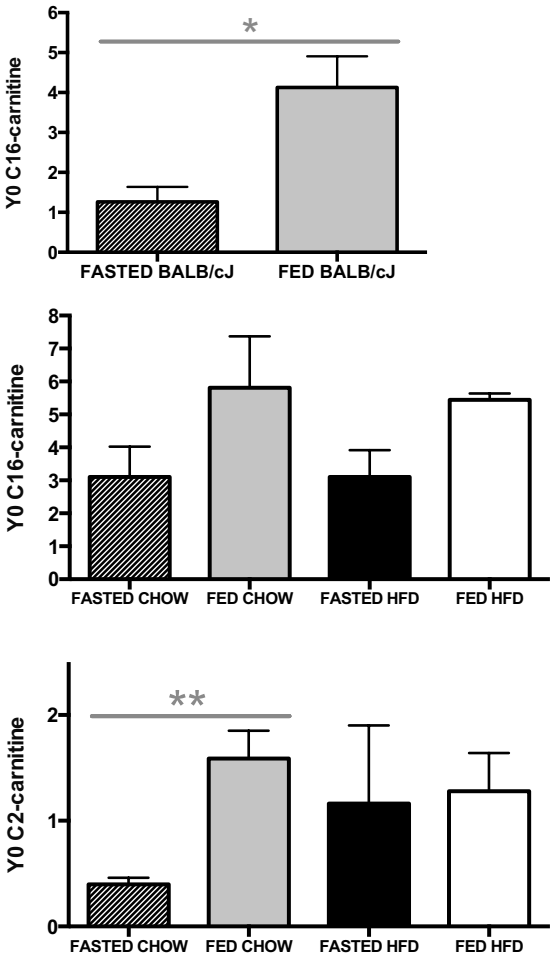

Figure 1 Y0 in fed versus fasted BALB/cJ and C57Bl6N mice (A) C16-carnitine Y0 in fed vs fasted BALB/cJ mice, (B) C16-carnitine Y0 and (C) C2-carnitine Y0 in fed vs fasted Bl6 mice. Data expressed as means ± SEM. P values < 0.05 are depicted as * and < 0.01 as **.

between fasted and fed BALB/cJ mice (p=0.004) and fasted and fed HFD C57BL/6N mice (p=0.008). For C2-carnitine we found ratios ranging from 15 in chow fed C57BL/6N mice to 149 in HFD fasted C57BL/6N mice (Supplemental figure S1b). Here the ratio was significantly greater in fasted chow C57BL/6N mice compared to fed (p=0.008), and in fed HFD C57BL/6N mice compared to fed chow mice (p=0.03).

The pool size of C16-carnitine in BALB/cJ mice was significantly greater in the fasted state compared to the fed (fed: 0.0040 µmol/mouse ± 0.0017 versus fasted: 0.0118 µmol/mouse ± 0.0021, p=0.0173)(figure 2a). In C57BL/6N mice, pool sizes of C16-carnitine did not differ between all groups (figure 2b). However for C2-carnitine, the pool size was significantly greater in fasted chow mice compared to fed chow mice (chow fed C2-carnitine pool size Q 0.14 µmol/mouse ± 0.03 and chow fasted C2-carnitine pool size Q 0.54

µmol/mouse ± 0.09, p=0.007)(figure 2c). There was no statistical difference between C2-carnitine pool sizes of HFD mice.

Elimination constant k (1/min)

K values were calculated by non-compartmental analysis of the TTR curves. In BALB/cJ mice, k values for C16-carnitine were overall much lower when compared to the k values for C16-carnitine in C57BL/6N mice (figure 3a and 3b) while the pool size of C16-carnitine was higher in BALB/cJ mice compared to C57BL/6N mice (figure 2a and 2b). Both in the BALB/cJ mice and the C57BL/6N mice the k values for C16-carnitine did not differ, meaning that HFD or fasting does not affect the capacity for eliminating or processing C16-carnitine in both BALB/cJ and C57BL/6N mice (figure 3a and 3b). However for C2-carnitine the fasting intervention did have a significant effect on the k value in the

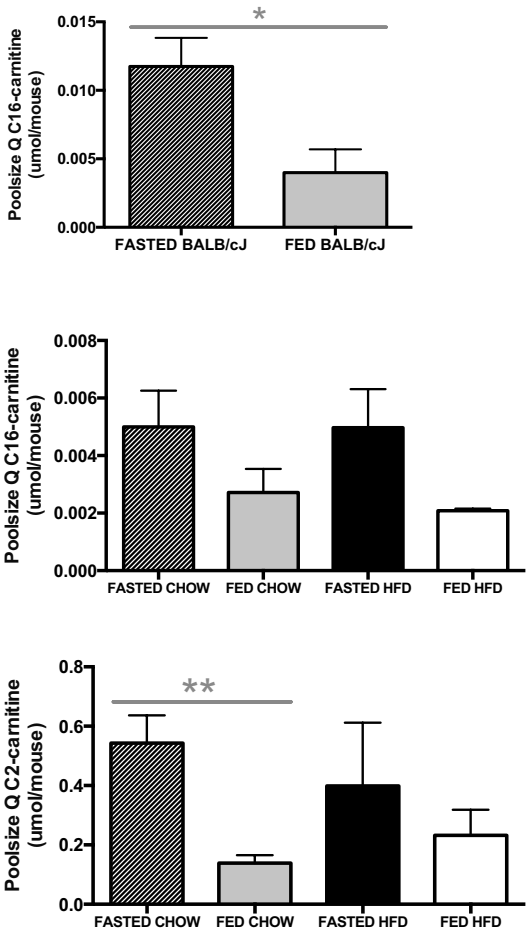

Figure 2 Poolsize Q in fed versus fasted BALB/cJ and C57Bl6N mice. (A) C16-carnitine poolsize (umol/mouse) in fed vs fasted BALB/cJ mice, (B) C16-carnitine poolsize and (C) C2-carnitine poolsize in fed vs fasted Bl6 mice.

chow fed animals, where k values decreased significantly (fed chow: k 0.18 ± 0.01 vs. fasted-chow: k 0.11 ± 0.01, p=0.016) (figure 3c). In HFD mice no difference in k values upon fasting was detected (fed HFD: k 0.15 ± 0.02 and fasted HFD: k 0.10 ± 0.02).

Rate of C16 and C2-carnitine appearance

The Ra for C16-carnitine was overall lower in BALB/cJ mice and C57BL/6N mice when compared to the Ra for C2-carnitine in C57BL/6N mice (figure 4a, b and c). As for the k values (elimination constant), both in BALB/cJ mice and C57BL/6N mice the Ra for C16-carnitine was unchanged by the fasting or diet intervention (figure 4a and 4b). However, in C57BL/6N mice the Ra for C16-carnitine trended towards higher levels in fasted mice. The Ra of C2-carnitine was significantly greater in chow fasted compared to chow fed C57BL/6N mice (fasted chow Ra: 0.05 µmol/min ± 0.01 versus fed chow Ra: 0.02

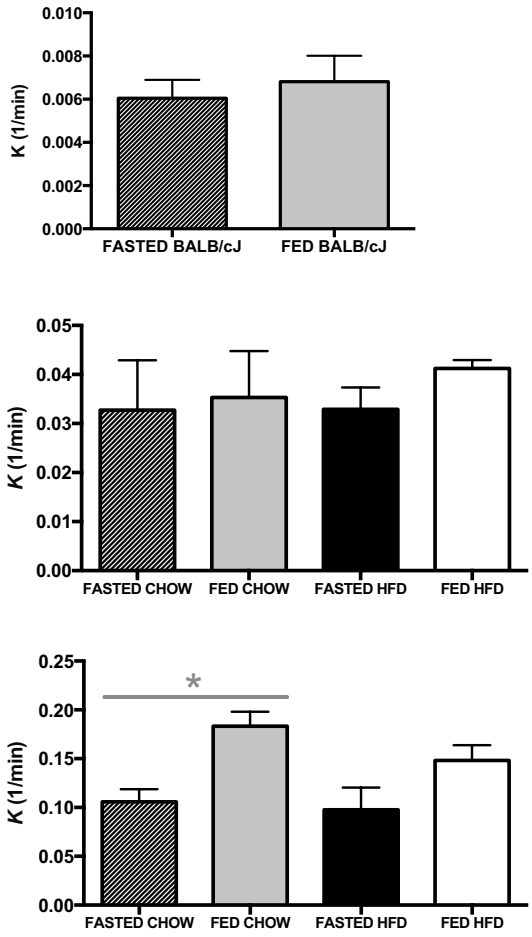

Figure 3 Elimination of acylcarnitine (A) Elimination constant k of C16-carnitine in lean BALB/cJ mice, and in (B) lean and obese C57Bl6N mice. (C) Elimination constant k of C2-carnitine in lean and obese C57Bl6N mice.

µmol/min ± 0.00, p=0.008), and also compared to fasted HFD C57BL/6N mice (fasted HFD Ra: 0.02 µmol/min ± 0.01, p=0.02)(figure 4c). This suggests that fasting promotes the appearance of C2-carnitine in chow mice, but this effect is diminished in HFD mice.

Curve fitting and modelling

In the BALB/cJ mice the TTR curves were mono-exponential with a very flat slope, making the curves to appear linearly shaped. This implies that the concentration of the tracee only marginally influences the uptake or disposal rate (Curves not shown). For C57BL/6N mice, we found exponentially shaped curves for both C16- and C2-carnitine (Curves not shown). This points towards fractional uptake of the tracee, where high plasma concentrations increase uptake (or disposal) as well. The curves of all mice showed single compartment decay. As acylcarnitines are proven to be exchanged between plasma and tissues (14, 29, 30), this single compartment decay means that the plasma compartment might act as a single compartment together with the interstitium and the cell cytosol of tissues.

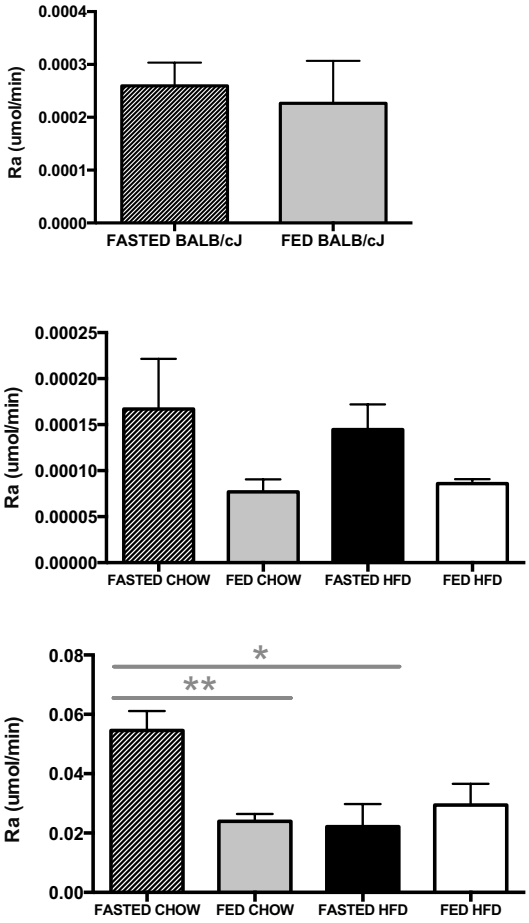

Figure 4 Rate of appearance (Ra) of acylcarnitines (A) Ra of C16-carnitine in lean BALB/cJ mice, and in (B) lean and obese C57Bl6N mice. (C) Ra of C2-carnitine in lean and obese C57Bl6N mice.

Discussion

Here, we describe for the first time C2- and C16-carnitine kinetics using a stable isotope tracer approach. In our tracer experiments we compared two mouse strains, BALB/cJ, known for its resistance against diet-induced glucose intolerance and derangements in lipid metabolism and C57BL/6N mice (26, 31). We analysed C2- and C16-carnitine with a single pool model, and showed that fasting and HFD did not affect C16-carnitine kinetics in BALB/cJ and C57BL/6N mice, but did affect C2-carnitine-kinetics in chow fed C57BL/6N mice. These effects were absent in HFD mice, indicating that HFD alters C2-carnitine metabolism.

Measurements of the initial enrichment showed that in fasted BALB/cJ mice the enrichment was lower, meaning that the pre-existing endogenous C16-carnitine pool must have been greater in fasted compared to fed mice. This was confirmed by a significantly greater pool size Q in fasted BALB/cJ mice, which also corresponds with our assumptions that the C16-carnitine pool is larger under fasted conditions, as FAO rates will be higher when glucose oxidation rates are lower due to fasting (12). This greater C16-carnitine pool size fits with higher C16-carnitine concentrations in plasma and some tissues of fasted BALB/cJ mice (i.e. liver, WAT but not muscle) (12). Additionally, the ratio between the anticipated pool and the actual pool was greatest in fasted BALB/cJ mice. This ratio reflects the proportion of the whole body pool size in relation to the calculated plasma pool size; thus a higher ratio reflects a higher proportion of ACs outside the plasma compartment. Therefore, the whole body C16-carnitine pool is larger in fasted BALB/cJ mice than in fed BALB/cJ mice. However, in C57BL/6N mice, fasting and HFD pool sizes trended towards higher levels but did not reach significance. This may illustrate differences in FAO rate or its efficiency since BALB/cJ and C57BL/6N mice differ in insulin sensitivity. When we compare these results with our study on correlations between plasma and tissue acylcarnitine profiles, we did find an increase of C16-carnitine concentrations in plasma and certain tissues (such as liver and WAT, but not muscle) of fasted C57BL/6N mice (12). This could imply that the pool size did not change upon fasting, but that there was a shift towards the plasma compartment and some tissue compartments as well. Alternatively, our group size in the current study may have been too small to reach significance.

Although fasting or diet did not affect the C16-carnitine pool in C57BL/6N mice, the C2-carnitine pool was higher in fasted chow but not HFD C57BL/6N mice. This difference in C2-carnitine pool size could simply be a reflection of FAO rates, which may differ between the chow and HFD mice, given their differences in glucose tolerance (data not shown). Alternatively, the different C2-carnitine pool between fasted chow versus HFD mice can be explained by differences in oxidative substrates. The greater C2-carnitine pool size in fasted chow C57BL/6N mice is in agreement with C2-carnitine concentrations in plasma and almost all tissues (12). The acetyl-group of C2-carnitine can either be lipid- or carbohydrate derived since both FAO and CHO yield acetyl-CoA as substrate (32). As the contribution of either FAO or CHO to the acetyl-CoA concentration can vary between insulin sensitive versus insulin resistant conditions, we assume that the difference

in C2-carnitine pool size is caused by a difference in oxidized substrate in the chow and HFD C57Bl/6N mice.

Interestingly in BALB/cJ mice, the elimination of C16-carnitine from the pool was overall much lower when compared to C57Bl6N mice. This demonstrates that elimination of acylcarnitines is not influenced by the size of the total pool, which was greater in BALB/cJ mice. This suggests that these insulin sensitive mice eliminate less C16-carnitine than the C57BL/6N mice, which are more prone to develop insulin resistance upon fasting. Additionally, both interventions of fasting and HFD did not affect the elimination rate of C16-carnitine, meaning that conditions of insulin resistance per sé do not determine elimination rates by tissue. This demonstrates that C16-carnitine is not eliminated from the pool with the purpose of being an energy substrate. Additionally the C16-carnitine TTR curves of the BALB/cJ mice were all almost linearly shaped, supporting that the C16-carnitine disposal is almost independent of the concentration. However we should consider that the elimination of C16-carnitine might also depend on the presence of other long-chain acylcarnitines using the same transporters as C16-carnitine. Thus, concentrations of both C16-carnitine and that of other long-chain acylcarnitines might influence elimination rates.

The exponential shape of the C16- and C2-carnitine TTR curves of C57BL/6N mice suggests concentration-driven elimination of the tracee. According to our current knowledge, no transporter is known for C16-carnitine on the cell membrane. For C2-carnitine the elimination rate was lower in fasted chow C57BL/6N mice compared to their fed counterparts. Assuming that in these fasted chow mice FAO rates were higher than in fed mice, this might indicate that the greater elimination of C2-carnitine in fed mice was mainly CHO driven. This would also explain why we did not find this difference in HFD fed mice. Here impaired metabolic flexibility could cause persistently higher FAO rates in the fed mice, and less elimination of C2-carnitine. Interestingly an inverse relation between lipid oxidation and C2-carnitine was suggested by Ebeling et al., supporting our assumptions on C2-carnitine elimination (32).
In concert with these findings on the elimination rates, the Ra of C16-carnitine was much lower than the Ra of C2-carnitine. This again underlines the quantitative importance of C2-carnitine, which might be distributed as either an energy substrate for the oxidation of acetyl-CoA, or a preferential way of distributing carnitine towards tissues. As for the elimination rates, we found no effect in general of both fasting and the diet for the Ra for C16-carnitine. Hence, production or release of C16-carnitine is not stimulated by insulin resistant or CHO-depleted conditions. The Ra for C2-carnitine was greater in fasted chow C57BL/6N mice than in the fed. Together with the elimination rates, this reflects more production rather than uptake of C2-carnitine in the fasted state, and more uptake rather than production in the fed state. Again, in HFD mice this difference was not detected, pointing at impaired substrate switching in these insulin resistant mice.
In addition to the elimination rates, TTR curves in all mice showed single compartment decay for both C16- and C2-carnitine. Because the total pool size was much greater

than the anticipated plasma pool, this implies that the plasma compartment forms one fast-exchanging pool with both interstitium and tissues. Probably, the exchange of acylcarnitines between plasma and tissue is continuous and not driven by gradients, suggesting that the borders of this single pool lie at the mitochondrial membrane where CPT-1 and CPT-2 attach and detach CoA-groups in exchange of carnitine and vice versa (13). On the other hand, large differences exist between plasma and tissue concentrations, e.g. muscle tissue contains more than 100 times the amounts of acylcarnitines compared to plasma (12). It is likely that a large part of whole body acylcarnitine content resides intra-mitochondrial.

A limitation of the current study was the administered tracer amount. In all experiments the TTR values were high, indicating that we have exceeded the tracer dosage, which should be aimed at in tracer studies. However, the whole body acylcarnitine pool is much larger than the fraction in plasma (Supplemental figure 1a and 1b), so it is unlikely that the infused tracer dosage has influenced whole body acylcarnitine metabolism.

In summary, we have shown here that the kinetics of C16- and C2-carnitine differ, and that this might illustrate their different roles. In addition we showed that the two mouse strains show different kinetics as well, probably due to their differences in insulin sensitivity and lipid metabolism (26, 31). We demonstrated that C16-carnitine kinetics may reflect C16-carnitine as a by-product of FAO. In contrast, C2-carnitine kinetics showed that C2-carnitine is a- quantitatively more present and b- more dependent on the metabolic state. Here C2-carnitine might function as a carnitine disposer or alternatively an oxidative substrate, which deserves more attention regarding its role in substrate switching and regulating glucose tolerance.

References

1. Wanders R, Vreken P, den Boer M, Wijburg F, Van Gennip A, Ijlst L. Disorders of mitochondrial fatty acyl-CoA beta-oxidation. Journal of Inherited Metabolic Disease. 1999;22(4):442-87.
2. Chegary M, Brinke H, Ruiter JP, Wijburg FA, Stoll MS, Minkler PE, et al. Mitochondrial long chain fatty acid beta-oxidation in man and mouse. Biochim Biophys Acta. 2009;1791(8):806-15.
3. Houten SM, Wanders RJ. A general introduction to the biochemistry of mitochondrial fatty acid beta-oxidation. J Inherit Metab Dis. 2010;33(5):469-77.
4. van Vlies N, Tian L, Overmars H, Bootsma A, Kulik W, Wanders R, et al. Characterization of carnitine and fatty acid metabolism in the long-chain acyl-CoA dehydrogenase-deficient mouse. Biochemical Journal. 2005;387(1):185-93.
5. Muoio DM, Koves TR. Lipid-induced metabolic dysfunction in skeletal muscle. Novartis Found Symp. 2007;286:24-38.
6. Koves TR, Ussher JR, Noland RC, Slentz D, Mosedale M, Ilkayeva O, et al. Mitochondrial overload and incomplete fatty acid oxidation contribute to skeletal muscle insulin resistance. Cell Metab. 2008;7(1):45-56.
7. An J, Muoio DM, Shiota M, Fujimoto Y, Cline GW, Shulman GI, et al. Hepatic expression of malonyl-CoA decarboxylase reverses muscle, liver and whole-animal insulin resistance. Nat Med. 2004;10(3):268-74.
8. Noland RC, Koves TR, Seiler SE, Lum H, Lust RM, Ilkayeva O, et al. Carnitine insufficiency caused by aging and overnutrition compromises mitochondrial performance and metabolic control. J Biol Chem. 2009;284(34):22840-52.
9. Mihalik SJ, Goodpaster BH, Kelley DE, Chace DH, Vockley J, Toledo FG, et al. Increased levels of plasma

acylcarnitines in obesity and type 2 diabetes and identification of a marker of glucolipotoxicity. Obesity (Silver Spring). 2010;18(9):1695-700.
10. Schooneman MG, Vaz FM, Houten SM, Soeters MR. Acylcarnitines: Reflecting or Inflicting Insulin Resistance? Diabetes. 2013;62(1):1-8.
11. Soeters MR, Sauerwein HP, Duran M, Wanders RJ, Ackermans MT, Fliers E, et al. Muscle acylcarnitines during short-term fasting in lean healthy men. Clin Sci (Lond). 2009;116(7):585-92.
12. Schooneman MG, Achterkamp N, Argmann CA, Soeters MR, Houten SM. Plasma acylcarnitines inadequately reflect tissue acylcarnitine metabolism. Biochim Biophys Acta. 2014.
13. Vaz FM, Wanders RJA. Carnitine biosynthesis in mammals. Biochemical Journal. 2002;361(3):417-29.
14. Ohashi R, Tamai I, Yabuuchi H, Nezu J-I, Oku A, Sai Y, et al. Na+-Dependent Carnitine Transport by Organic Cation Transporter (OCTN2): Its Pharmacological and Toxicological Relevance. Journal of Pharmacology and Experimental Therapeutics. 1999;291(2):778-84.
15. Tamai I, Ohashi R, Nezu J, Yabuuchi H, Oku A, Shimane M, et al. Molecular and functional identification of sodium ion-dependent, high affinity human carnitine transporter OCTN2. J Biol Chem. 1998;273(32):20378-82.
16. Holland WL, Knotts TA, Chavez JA, Wang LP, Hoehn KL, Summers SA. Lipid mediators of insulin resistance. Nutr Rev. 2007;65(6 Pt 2):S39-S46.
17. Shulman GI. Cellular mechanisms of insulin resistance. The Journal of Clinical Investigation. 2000;106(2):171-6.
18. Morino K, Petersen KF, Shulman GI. Molecular mechanisms of insulin resistance in humans and their potential links with mitochondrial dysfunction. Diabetes. 2006;55 Suppl 2:S9-S15.
19. Pouteau E, Nguyen P, Ballevre O, Krempf M. Production rates and metabolism of short-chain fatty acids in the colon and whole body using stable isotopes. The Proceedings of the Nutrition Society. 2003;62(1):87-93.
20. Meissner M, Herrema H, van Dijk TH, Gerding A, Havinga R, Boer T, et al. Bile acid sequestration reduces plasma glucose levels in db/db mice by increasing its metabolic clearance rate. PLoS One. 2011;6(11):e24564.
21. Mittendorfer B, Liem O, Patterson BW, Miles JM, Klein S. What does the measurement of whole-body fatty acid rate of appearance in plasma by using a fatty acid tracer really mean? Diabetes. 2003;52(7):1641-8.
22. Deutz NE, Bruins MJ, Soeters PB. Infusion of soy and casein protein meals affects interorgan amino acid metabolism and urea kinetics differently in pigs. J Nutr. 1998;128(12):2435-45.
23. Ramos-Roman MA, Sweetman L, Valdez MJ, Parks EJ. Postprandial changes in plasma acylcarnitine concentrations as markers of fatty acid flux in overweight and obesity. Metabolism. 2012;61(2):202-12.
24. Muoio DM, Noland RC, Kovalik JP, Seiler SE, Davies MN, DeBalsi KL, et al. Muscle-Specific Deletion of Carnitine Acetyltransferase Compromises Glucose Tolerance and Metabolic Flexibility. Cell Metabolism. 2012;15(5):764-77.
25. Seiler SE, Martin OJ, Noland RC, Slentz DH, Debalsi KL, Ilkayeva OR, et al. Obesity and lipid stress inhibit carnitine acetyltransferase activity. J Lipid Res. 2014;55(4):635-44.
26. Farrell GC, Mridha AR, Yeh MM, Arsov T, Van Rooyen DM, Brooling J, et al. Strain dependence of diet-induced NASH and liver fibrosis in obese mice is linked to diabetes and inflammatory phenotype. Liver international : official journal of the International Association for the Study of the Liver. 2014;34(7):1084-93.
27. Montgomery MK, Hallahan NL, Brown SH, Liu M, Mitchell TW, Cooney GJ, et al. Mouse strain-dependent variation in obesity and glucose homeostasis in response to high-fat feeding. Diabetologia. 2013;56(5):1129-39.
28. Wolfe RRCDL. Isotope Tracers in Metabolic Research: Principles and Practice of Kinetic Analysis. 2nd ed. Hoboken, New Jersey: John Wiley & Sons; 2005.
29. Ramsay RR, Gandour RD, van der Leij FR. Molecular enzymology of carnitine transfer and transport. Biochim Biophys Acta. 2001;1546(1):21-43.
30. Tamai I, Ohashi R, Nezu Ji, Yabuuchi H, Oku A, Shimane M, et al. Molecular and Functional Identification of Sodium Ion-dependent, High Affinity Human Carnitine Transporter OCTN2. Journal of Biological Chemistry. 1998;273(32):20378-82.
31. Fearnside JF, Dumas ME, Rothwell AR, Wilder SP, Cloarec O, Toye A, et al. Phylometabonomic patterns of adaptation to high fat diet feeding in inbred mice. PLoS One. 2008;3(2):e1668.
32. Ebeling P, Tuominen JA, Arenas J, Garcia Benayas C, Koivisto VA. The association of acetyl-L-carnitine with glucose and lipid metabolism in human muscle in vivo: the effect of hyperinsulinemia. Metabolism. 1997;46(12):1454-7.

Supplemental data

Figure S1 Ratios pool size and anticipated poolsize of (A) C16-carnitine and (B) C2-carnitine.

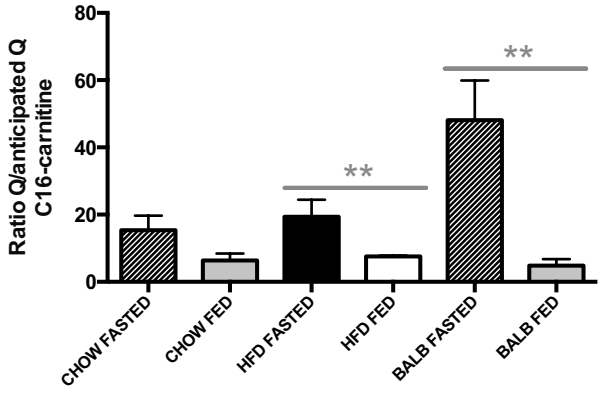

Figure S1a

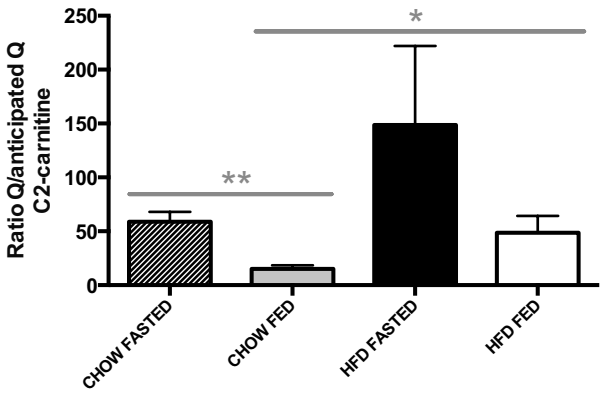

Figure S1b